Studies of nitride- and oxide-based materials as absorptive shifters for embedded attenuated phase-shifting mask in 193 nm

Cheng-ming Lin, Keh-wen Chang, Ming-der Lee and Wen-an Loong

Institute of Applied Chemistry, National Chiao Tung University
Hsin-Chu 300, Taiwan, Republic of China

ABSTRACT

Abstract-Five materials which are $PdSi_xO_y$, $CrAl_xO_y$, SiN_x, $TiSi_xN_y$ and $TiSi_xO_yN_z$ as absorptive shifters for attenuated phase-shifting mask in 193 nm wavelength lithography are presented. $PdSi_xO_y$ films were deposited by dual e-gun evaporation. $CrAl_xO_y$, $TiSi_xN_y$ and $TiSi_xO_yN_z$ films were formed by plasma sputtering and SiN_x films were formed with LPCVD. All of these materials are shown to be capable of achieving 4%~15% transmittance in 193 nm with thickness that produce a 180° phase shift. Under BCl_3:Cl_2=14:70 sccm; chamber pressure 4 mtorr and RF power 1900W, the dry etching selectivity of $TiSi_xN_y$ over DQN positive resist and fused silica, were found to be 2:1 and 4.8:1, respectively. An embedded layer $TiSi_xN_y$ with 0.5 μm line/space was successfully patterned.

1. INTRODUCTION

We have reported several Ti-based materials as new embedded materials for AttPSM [1-3]. Here we presented $PdSi_xO_y$, $CrAl_xO_y$, SiN_x, $TiSi_xN_y$ and $TiSi_xO_yN_z$ as embedded materials for AttPSM in 193 nm. $PdSi_xO_y$ films were deposited by dual e-gun evaporation. $CrAl_xO_y$, $TiSi_xN_y$ and $TiSi_xO_yN_z$ films were formed by plasma sputtering and SiN_x formed with LPCVD.

2. EXPERIMENTAL

$PdSi_xO_y$ was formed with dual e-gun evaporation of Pd and SiO_2 targets under chamber pressure 1×10^{-6} torr. $CrAl_xO_y$ was formed by plasma sputtering of Cr (30~50 W) and Al (40 W) under Ar (30 sccm) and discontinuous O_2 0.5 sccm with an Ion Tech Merovac 450C sputtering system. $TiSi_xN_y$ films were formed by plasma sputtering of Ti (180~230 W) and Si (60~80 W) under Ar (50 sccm) and N_2 (4~6 sccm). $TiSi_xO_yN_z$ was also formed by plasma sputtering of Ti (200~240 W) and Si (60~80 W) under Ar (50 sccm), N_2 (4~6 sccm) and O_2 (0.2~0.7 sccm). However, SiN_x was deposited by LPCVD under $SiCl_2H_2$ (98~105 sccm), NH_3 (22~35 sccm), chamber pressure 150 mtorr and 750~850℃. The deposition rate of these thin films was 3~11.2 nm/min.

Transmittance T% and reflectance R% were taken from a Shimadsu UV-2501PC double-beam UV-VIS spectrometer. Thickness was measured using a Dektak 3030 surface profilometer and a n&k Technology NKT 1200 analyzer. The ion depth profiles of these thin films were analyzed by a Cameca IMS-5F secondary ion mass spectrometer (SIMS) using O_2^+ as ion source under 12.5 kV and 20,000 mass resolution power. Sheet resistance was measured using a Napson RT-7 resistance analyzer. Micrographs were taken by a Hitachi S-400 FE-SEM and a Hitachi S-6260H in-line CCFE-SEM. The chemical composition of thin film surface was analyzed with a VG Microlab 310F Electron Spectroscopy for Chemical Analysis (ESCA) using Mg K_α standard source under scan 1 eV.

The etching selectivity of embedded materials over fused silica and DQN positive resist was achieved with an Anelva ILD-4100 helicon wave etcher and a Vacutec AB 1500S RIE.

3. RESULTS AND DISCUSSION

The thin film's R% and T% in 193 nm were measured, and their n and k were calculated with our modified R-T Method [3]. The R% in the range of 190~200 nm wavelength changed quite sharply, the value of R% in 193 nm is therefore not very reliable, and will effect the correct determination of n and k. The related optical properties are shown in Table 1.

Part of the SPIE Conference on Optical Microlithography XII • Santa Clara, California • March 1999
SPIE Vol. 3679 • 0277-786X/99/$10.00

Downloaded From: http://proceedings.spiedigitallibrary.org/ on 04/28/2014 Terms of Use: http://spiedl.org/terms

3. 1. $PdSi_xO_y$

Optical Properties: The percentage of Pd in $PdSi_xO_y$ film which was estimated by its thickness during coating is critical to the film's n and k as shown in Fig. 1. If the percentage of Pd thickness [$Pd/(Pd+SiO_2)$] was kept in the range of 25%~38%, then the T% at visible wavelength (488, 632.8 nm) is 35~50% at calculated thickness d_{180} (thickness required for phase shift of 180°), suitable for optical alignment. When the percentage of Pd thickness is higher than 40%, T% at 193 nm is lower than 1.7% with the thickness d_{180}, no longer suitable as embedded material. When the percentage of Pd thickness is lower than 15%, SiO_2-like structure became the major component of $PdSi_xO_y$ film. The T% at visible wavelength will rise to 60~75%, hence, no longer suitable for optical alignment. With 30% Pd thickness, a sheet resistance R_s of 76.7 Ω/square for $PdSi_xO_y$ was measured. The conductivity is acceptable for e-beam patterning.

Physical and Chemical Properties: The SiO_2-like structure existed in $PdSi_xO_y$ film, so this film has a good resistance to strong acid as shown in table 2. ESCA analyses demonstrated the existence of PdSi chemical structures in $PdSi_xO_y$, and this structure has been proved to have good conductivity, could reduce charging effect during e-beam direct-write. Since the expensive ArF 193 nm laser is not available, a ~254 nm broad band deep ultraviolet light was used instead to examine the exposure durability of these thin films. Irradiation dosage up to 2×10^2 J/cm^2, the optical properties of $PdSi_xO_y$ films showed only a very slight change.

Etching Selectivity: The conditions, $NF_3:Cl_2$=45:5 sccm, O_2 10 sccm, chamber pressure 100 mtorr and RF power 200W were used for the etching of $PdSi_xO_y$ film. The results indicated that the etching selectivity of $PdSi_xO_y$ over resist was 0.02:1, over fused silica was 1:0.7. This etching selectivity is not suitable for the embedded material. Further studies on etching are needed.

3. 2. $CrAl_xO_y$

Optical Properties: In order to decrease oxide structure, the O_2 flow was limited to less than 1 sccm during deposition of $CrAl_xO_y$ films. The increasing of power of Cr target will increase the n and k of $CrAl_xO_y$ films as illustrated in Fig. 2. The power of Al target was limited to less than 45 W during sputtering, however, Al/Cr ratio must be higher than 1.9 in $CrAl_xO_y$ to show good optical properties [4]. A discontinuous flow (stop/flow) of O_2 0.5 sccm was used to deposit $CrAl_xO_y$ to form multi-layer film and to increase Al content by DC plasma sputtering of Cr (30~40 W) and Al (40 W) under Ar 30 sccm. The decreasing of time ratio of O_2 flow will increase both the n and k of $CrAl_xO_y$ as shown in Fig. 3.

Physical and Chemical Properties: The tensile stress is in the range of 150~600 MPa for $CrAl_xO_y$ films by traced stress measurements and is in acceptable range. The SIMS of $CrAl_xO_y$ films indicated the presence of swing curves for Cr, O and Al atoms as shown in Fig. 4. The swing curves proved the formation of multi-layer film by plasma sputtering deposition under Ar and discontinuous oxygen (flow on and off). Table 2 listed the results of four different methods and solutions for testing the cleaning durability of $CrAl_xO_y$ films. The T% in 193 nm for $CrAl_xO_y$ films by using the first two methods has changed greatly. Because of Al structure existing in $CrAl_xO_y$ films, it could be dissolved in strong acidic and basic solutions. Fortunately, the next two methods, DI water with ultrasonic and Microstrip solution, could be used to do the clean of $CrAl_xO_y$. Using Cl_2 RIE and Taguchi Method to etch the $CrAl_xO_y$ films, the etching selective ratio to substrate SiO_2 were found to be 4:1

Etching Selectivity: The plasma etching rate and selectivity were studied with several chlorine-based gases such as BCl_3 and Cl_2. The conditions of $BCl_3:Cl_2$=5:20 sccm, chamber pressure 4 mtorr and RF power 1400W were carried out for $CrAl_xO_y$ film etching. The results indicated that the etching rate of $CrAl_xO_y$ embedded layer was 28~36Å/sec, the etching selectivity of $CrAl_xO_y$ over resist was 1.5:1, a little lower than expected; over fused silica was 3.1:1.

3. 3. SiN_x

Optical Properties: Deposition of SiN_x films with $SiCl_2H_2$ and NH_3 gases by the method of LPCVD instead of sputtering and PECVD to form embedded layer is first reported by this paper. Si atom increased in SiN_x films with the increasing of $SiCl_2H_2$ flow, k also increased while n changed only very slightly.

Physical and Chemical Properties: Because of SiN_x deposited at 750~850℃, it's stable during the examination of thermal durability by annealing up to 250℃ and holding for one hour. After the test of cleaning durability by four methods as shown in table 2, the T% at 193 nm changes slightly, therefore, the film has good chemical durability. SiN_x films from LPCVD have more stable compositions than PECVD or sputtering.

Downloaded From: http://proceedings.spiedigitallibrary.org/ on 04/28/2014 Terms of Use: http://spiedl.org/terms

Etching Selectivity: The selective ratios to substrate SiO_2 were found to be 5:1 by Cl_2 RIE.

3. 4. $TiSi_xN_y$

Optical Properties: When N_2 flow was kept in 4~6 sccm, the T% at visible wavelength is 35~50%, suitable for optical alignment. If N_2 flow lower than 4 sccm, the T% will rise to 60~75%, no longer suitable for optical alignment. When N_2 flow is higher than 7 sccm, $TiSi_xN_y$ films will not have reasonable conductivity, might have charging effect during e-beam direct-write. Under N_2 flow 4 sccm, 12.5 kΩ/square R_s was measured. The conductivity is acceptable for e-beam patterning.

Physical and Chemical Properties: After the irradiation by a ~254 nm broad band deep-UV light up to 2×10^3 J/cm^2, optical properties of $TiSi_xN_y$ thin films change only slightly.

Etching Selectivity: The conditions of BCl_3:Cl_2=14:70sccm, chamber pressure 4 mtorr and RF power 1900W were carried out for $TiSi_xN_y$ films. The results indicated that the etching selectivity of $TiSi_xN_y$ over resist was 2:1, over fused silica was 4.8:1.

3. 5. $TiSi_xO_yN_z$

Optical Properties: Compared to $TiSi_xN_y$ as shown in Table 1, $TiSi_xO_yN_z$ layer has lower values of n, k and R% in 193 nm.

Physical and Chemical Properties: MAC MX-3 X-ray Diffractometer (XRD) was used to analyze $TiSi_xO_yN_z$ thin films and an amorphous structure was confirmed for these films.

Table 1. Optical properties in 193 nm

	193 nm				488 nm[b]	632.8 nm[b]
	Calculated thickness d_{180}	n, k	T%, R%	Phase shift by interfaces[a]	T%, R%	T%, R%
$PdSi_xO_y$	96.1 nm	2.01, 0.45	5.1%, 12.6%	-2.98°	35.8%, 14.4%	46.5%, 20.6%
$CrAl_xO_y$	80.5 nm	2.21, 0.41	9.5%, 14.4%	-3.01°	82.1%, 17.2%	80.5%, 18.6%
SiN_x	72.6 nm	2.33, 0.46	9.1%, 17.1%	-3.51°	76.1%, 28.2%	78.1%, 26.8%
$TiSi_xN_y$	84.7 nm	2.14, 0.48	5.8%, 14.3%	-3.45°	36.1%, 22.1%	45.3%, 25.7%
$TiSi_xO_yN_z$	101.6 nm	1.95, 0.42	5.3%, 11.6%	-2.78°	40.5%, 25.2%	49.7%, 17.2%

[a] Refractive index of quartz 1.56 under 193 nm wavelength was used.
[b] Wavelength for inspection and alignment.

Table 2. The change of T% in 193 nm after the test of cleaning durability

	H_2SO_4-H_2O_2 (3:1) solution at 80℃, 30 min	NH_4OH-H_2O_2-H_2O (1:2:7) solution at 80℃, 30 min	DI water with ultrasonic at 80℃, 30 min	Microstrip 2001 solution at 80℃, 30 min
$PdSi_xO_y$	+ 0.4	N. A.	N. A.	N. A.
$CrAl_xO_y$	+ 5.2	+ 40.2	+ 0.2	+ 0.2
SiN_x	+ 0.2	– 0.3	+ 0.2	N. A.

3. 6. Phase Shift from Interfaces

Besides the embedded layer itself, the additional phase-shift contributed from interfaces could be calculated by [5]:

$$\phi = \arg\left(\frac{2n_2^*}{n_1^* + n_2^*}\right)$$

The all interfaces were found to generate totally about –3.45°, –2.78°, –3.51°, –3.01° and –2.98° phase-shift loss from $TiSi_xN_y$, $TiSi_xO_yN_z$, SiN_y, $CrAl_xO_y$ and $PdSi_xO_y$ on quartz substrate, respectively. The interface A which is between quartz and embedded layer alone contributed about 90% of loss of phase-shift as shown in Fig. 5. The degree of loss is not critical, however, the increasing of 1~2 nm of embedded layer's thickness to compensate this loss of phase-shift is suggested.

Downloaded From: http://proceedings.spiedigitallibrary.org/ on 04/28/2014 Terms of Use: http://spiedl.org/terms

3. 7. n, k Plane

The n, k plane of five compounds we studied was shown in Fig. 6 which including the window suitable to be used as embedded material in 193 nm. By controlling the sputtering or deposition conditions, the optical properties of these five compounds could be kept inside this window.

3. 8. Patterning

Because 0.25 inch thickness fused silica was too thick to be placed into the chamber of helicon wave etcher, SiO_2/Si wafer was replaced as substrate for $TiSi_xN_y$ embedded layer. Fig. 7 illustrated a 0.5μm line/space etched pattern of $TiSi_xN_y$ as embedded layer. The patterning of other materials has not been successfully so far.

4. CONCLUSIONS

Five films which are $PdSi_xO_y$, $CrAl_xO_y$, SiN_x, $TiSi_xN_y$ and $TiSi_xO_yN_z$ have potential to be used as good absorptive shifters (embedded layers) for AttPSM in 193 nm wavelength lithography. By controlling the films deposition conditions, a wide range of optical properties of these materials could be achieved. The drawback of $CrAl_xO_y$ and SiN_x films is their lower conductance. A thickness of 5 nm Cr film is added to bring down the sheet resistance of $CrAl_xO_y$ and SiN_x films to about 10 kΩ/□ which is suitable to reduce the charging effect during e-beam direct-write.

REFERENCES

1. W. A. Loong, T. C. Chen and J. C. Tseng, *Microelectronic Engineering*, ***30***, p. 157 (1996).
2. W. A. Loong, T. C. Chen, S. L. Shy, J. C. Tseng and R. J. Lin, *Proc. SPIE*, ***2726***, p. 524 (1996).
3. W. A. Loong, C. W. Chen, Y. H. Chang, C. M. Lin, Z. Cui and C. A. Lung, *Microelectronic Engineering*, ***41/42***, p. 125 (1998).
4. E. Kim et al., *Applied Optics*, ***37 (19)***, p. 4254 (1998).
5. B. W. Smith et al., *Microelectronic Engineering*, ***35***, p. 201 (1997).

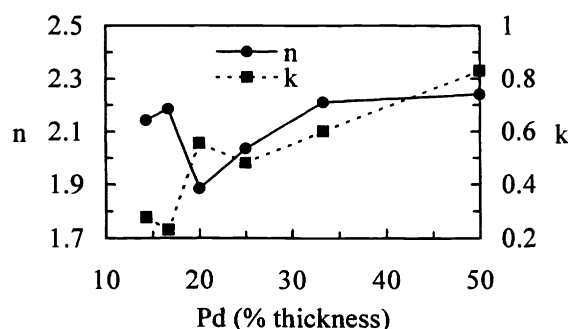

Fig. 1 The effect of percent of Pd thickness on n and k of $PdSi_xO_y$ films.

Downloaded From: http://proceedings.spiedigitallibrary.org/ on 04/28/2014 Terms of Use: http://spiedl.org/terms

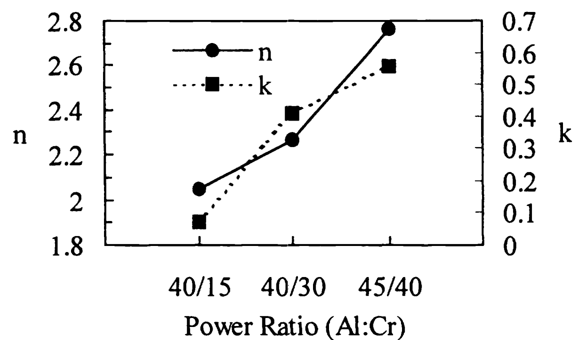

Fig. 2 The effect of power ratio between Al and Cr targets on n and k of $CrAl_xO_y$ films under Ar 60 sccm and O_2 1 sccm.

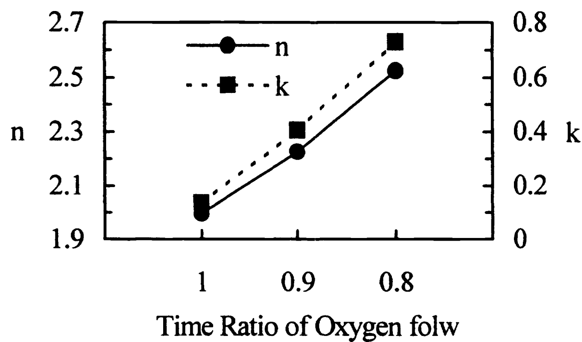

Fig. 3 The effect of time ratio of O_2 flow on n and k of multi-layer $CrAl_xO_y$ films under Al 40 W, Cr 40 W, Ar 30 sccm and O_2 0.5 sccm.

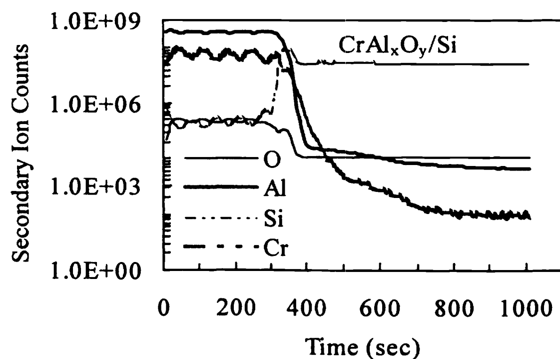

Fig. 4 SIMS of multi-layer $CrAl_xO_y$ film.

Downloaded From: http://proceedings.spiedigitallibrary.org/ on 04/28/2014 Terms of Use: http://spiedl.org/terms

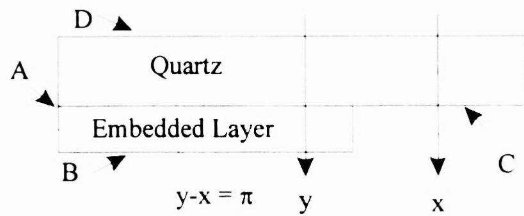

Fig. 5 Interfaces of AttPSM.

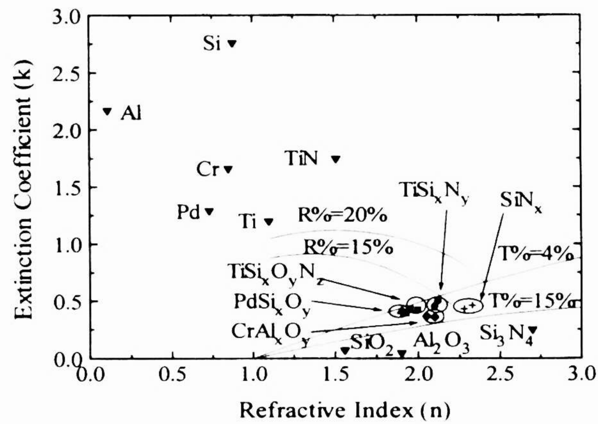

Fig. 6 n, k plane of five embedded materials under 193 nm wavelength.

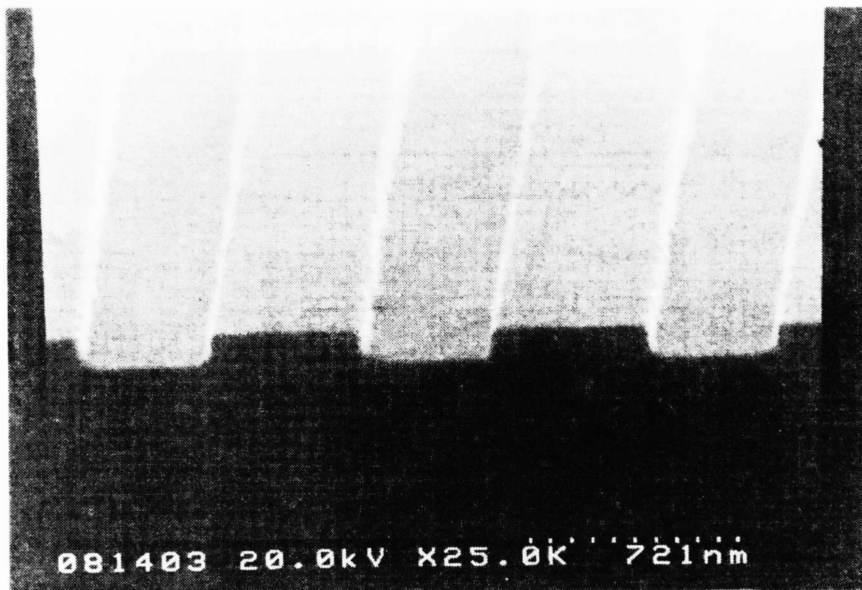

Fig. 7 SEM of a 0.5 μm line/space etched pattern of $TiSi_xN_y$ embedded layer on SiO_2/Si substrate.

Downloaded From: http://proceedings.spiedigitallibrary.org/ on 04/28/2014 Terms of Use: http://spiedl.org/terms